

# Radiative Transfer Modelling in Inhomogeneous Clouds by Means of the Monte Carlo Method

Sebastián Gimeno García and Thomas Trautmann

## Summary

The Monte Carlo (MC) method is an effective approach to simulate the radiative transfer in an inhomogeneous cloudy atmosphere. It is based on the direct physical simulation of the extinction processes that solar and thermal photons incur when traveling through the atmosphere. A detailed description of the MC method is presented in the second chapter. A new three-dimensional Monte Carlo radiative transfer model, based on a pre-existing model (*Trautmann et al.* [1999]), has been developed. Some outstanding characteristics of this model are discussed in chapter 3. Several simulations of reflectances, transmittances, absorptances and horizontal flux densities have been performed, the results of which have been compared with worldwide accepted codes (chapter 4). The two cases selected for the radiative transfer computations were taken from the Intercomparison of 3D Radiative Codes (I3RC) project: an ARM (Atmospheric Radiation Measurements) reconstructed cloud and a 3D marine boundary layer cloud.

## Zusammenfassung

Die Monte Carlo (MC) Methode ist ein effektives Verfahren, um den Strahlungstransport in einer inhomogenen bewölkten Atmosphäre zu simulieren. Es begründet sich auf der direkten Simulation der Extinktionsprozesse eines solaren oder thermischen Photons auf seinem Weg durch die Atmosphäre. Eine detaillierte Beschreibung der MC Methode erfolgt in Kapitel 2. In Kapitel 3 wird ein neues dreidimensionales MC-Strahlungstransportmodell vorgestellt, das, aufbauend auf einem schon bestehenden Modell (*Trautmann et al.* [1999]), entwickelt wurde. Mehrere Simulationen von Reflektanzen, Transmittanzen, Absorptanzen und Strahlungsflussdichten für zwei Fälle des "Intercomparison of 3D radiative Codes" projektes, nämlich eine ARM rekonstruierte Wolke und eine 3D marine Grenzschichtwolke, wurden durchgeführt, und mit den Ergebnissen anderer weltweit akzeptierten Codes verglichen.

## 1 Introduction

Recent research works (*Valero et al.* [1997], *Cess et al.* [1995]) have pointed out discrepancies between shortwave absorption by clouds inferred from the vertical net flux densities difference measurements and predicted by theoretical models. The traditional approach for a homogeneous plane-parallel cloud takes into account the vertical photon transfer only. In this case, absorption is only determined by vertical net flux differences, neglecting any horizontal energy transport. This is generally a rough approximation, since in reality clouds exhibit strong horizontal variability in both geometry and optical properties, inducing horizontal radiative transfer (in highly variable cloud or aerosol fields it can be of the same magnitude as that of vertical fluxes).

This discordance calls for a more realistic treatment of the atmospheric singularities in the theoretical approaches in order to throw light on the controversy opened. Many institutions and research centers, including the Institute of Meteorology of Leipzig, have

recently developed three-dimensional (3D) radiative transfer models to take the extinction field variability into consideration and to estimate the errors, when assuming 1D variability in the conventional computations.

There are basically two strategies to deal with the radiative transfer (RT) in the atmosphere:

1. numerically and/or analytically solving the integral or differential form of the radiative transfer equation (RTE), or
2. statistically and stochastically simulating the physical processes taking place between photons and atmospheric constituents (Monte Carlo Method, *Marchuk et al.* [1980]).

Both approaches have advantages and disadvantages, and the suitability of using one or the other depends on the particular case under investigation. In this paper we will focus on the description of the main characteristics of the MC method (chapter 2) as well as on some peculiarities of the Leipzig MC Model (LMCM) in the third chapter; leaving out of our discussion the RTE-solving methods.

The proliferation of independent RT models demanded a comparison of the models with each other, in order to check the validity of all of them and not induce more confusion. In 1999 began the Intercomparison of Three-Dimensional Radiative Codes (*I3RC*) project, with the goal of comparing a wide variety of 3D RT methods applied to Earth's atmosphere, with a few selected cloud fields as input, and a few selected radiative quantities as output. In chapter 4, we will present some results obtained with the LMCM for two cases of the Phase I of I3RC project, together with the results of worldwide accepted codes.

We will conclude with a few remarks about the LMCM and give an overview of the future (and present) work that will be (and is already) done in frame of the (*4DCLOUDS*) project.

## 2 The Monte Carlo Method

If we neglect diffraction, photons traveling through the atmosphere can only interact with the atmospheric molecules and particulates either by means of scattering or absorption. In this way, photons can only change flight direction after a scattering event. The MC method is based on the direct simulation of these physical processes.

Let us now explain in more detail the basis of the MC method. On one hand, a virtual atmosphere —with absorbing gases, cloud and aerosol fields, and the Earth's surface as the lowest boundary— is build up as the interacting medium. Then, a large number of photons are let to enter the atmosphere at the top (incoming solar photons). These photons will meet atmospheric particles during their trip, and sometimes they will talk to each other (interaction) and other times they will continue as nothing else than vacuum were in between. Photons can notice the presence of matter in different ways —molecular (Rayleigh) scattering, gaseous and particulate absorption, absorption and scattering by droplets and aerosols, etc—, and the particular one, that will actually take place, is randomly selected according to the cross sections (or extinction coefficients) of the different processes, or in other words, to the probabilities of the distinct ways of interaction. At the other hand, the medium is discretized in little cells of constant properties, conferring to the total atmosphere the appearance of a grid, where many virtual surfaces can be

considered. The MC approach sums up all the number of photons crossing virtual test surfaces and traveling in particular directions. With this information, the intensity as a function of position can be directly obtained. It also allows us to compute other relevant quantities such as fluxes, flux densities, the mean intensity fields, and heating rates due to absorption of photons within the medium, etc. Figure 1 shows a detailed scheme of the MC algorithm.

The MC method has advantages and disadvantages in comparison with the methods which are based on the numerical integration of the RTE.

One of its major advantages is the possibility of dealing with very complicated cloud structures. Generally, clouds used in 3D analytical simulations consist of simple geometrical shapes with constant liquid water content (LWC) distributed in one or few atmospheric layers. With the evolution of computational technologies, more realistic cloud fields derived from stochastic modeling methods, satellite imagery, microwave-radar measurements, etc., have been incorporated to radiative transfer models, and the MC method has no difficulty to account for inhomogeneities in the optical properties, in contrast to the RTE-solving approaches.

The MC method also offers the possibility of managing arbitrary complicated scattering phase functions. Actually, the more anisotropic the scattering process is, the faster is the MC method; as opposed to RTE-solving methods.

The main disadvantage of the MC method is the computational time expense that is necessary to achieve high accuracy, since accuracy depends on the number of photons used in the simulation.

## 2.1 Determination of Photon Paths

Let us assume that a photon —more precisely, a packet of photons— is located at a point  $\vec{r}_0$  where an extinction event takes place. Now, the photon will travel the distance  $l$  in the direction  $\vec{k} = (k_x, k_y, k_z)$  until the next extinction point  $\vec{r}$ . The new position of the photon can be expressed as a translation from  $\vec{r}_0$  to  $\vec{r}$  as follows:

$$\vec{r} = \vec{r}_0 + l \vec{k}, \quad (1)$$

where the distance  $l$  is calculated from the Bouguer-Lambert-Beer transmission law with the help of a random number  $R[0, 1)$ ,

$$T(l) = \exp(-\beta_{ext}l), \quad (2)$$

$$l = -\frac{1}{\beta_{ext}} \ln R[0, 1). \quad (3)$$

with  $\beta_{ext}$  being the volume extinction coefficient of the medium under consideration. In case of a discretized inhomogeneous medium (see figure 2), Eq. (2) must be written in a more general form,

$$T(l) = \exp\left[-\int_l \beta_{ext}(s) ds\right] \simeq \exp\left[-\sum_i \beta_{ext}^i l_i\right], \quad (4)$$

and  $l = \sum_i l_i$  is deduced from the following relation,

$$\sum_i \beta_{ext}^i l_i = -\ln R[0, 1), \quad (5)$$

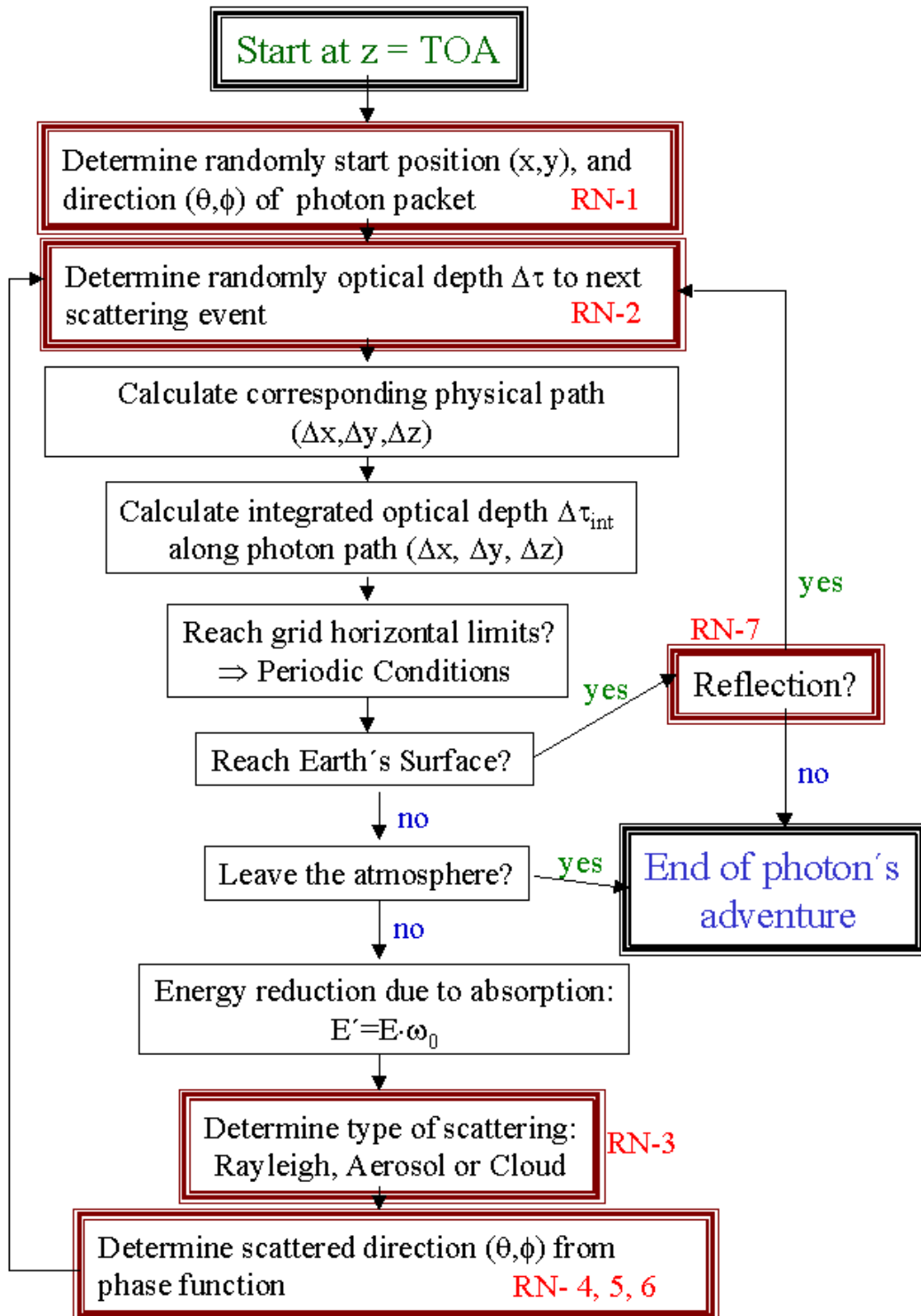
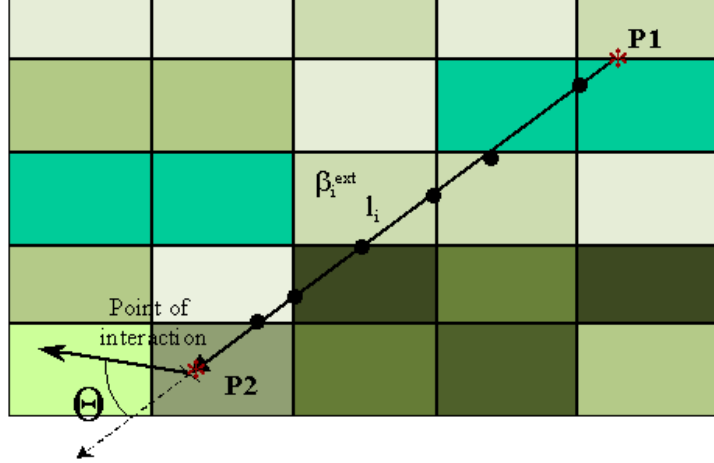


Figure 1: Scheme of the Monte Carlo Method



**Figure 2:** Scheme of photon transport in an inhomogeneous cloud. The different color tonalities of the atmospheric cells illustrate different extinction coefficients. The stars indicate the interaction events and the full points show the intersection points.

where  $\beta_{ext,i}$  and  $l_i$  are the volume extinction coefficient of the grid cell  $i$  and the path travelled through the cell  $i$ , respectively.

The photon flight direction after the scattering interaction  $\Omega = (\theta, \phi)$ , defined by the zenith  $\theta$  and the azimuthal angle  $\phi$ , results from a random process weighted with the scattering phase function  $p(\Omega, \Omega_0)$ , where  $\Omega_0 = (\theta_0, \phi_0)$  refers to the incident direction:

$$\int_0^\theta p(\Omega, \Omega_0) \sin \theta d\theta = R[0, 1) \int_0^\pi p(\Omega, \Omega_0) \sin \theta d\theta, \quad (6)$$

$$\int_0^\phi p(\Omega, \Omega_0) d\phi = R[0, 1) \int_0^{2\pi} p(\Omega, \Omega_0) d\phi. \quad (7)$$

After some algebra that is beyond the scope of this article, the new flight direction  $\vec{k}$  can be expressed in terms of the preceding direction  $\vec{k}'$ , as follows:

$$k_x = k'_x \cos \theta - h (k'_y \sin \phi + k'_x k'_z \cos \phi) \quad (8)$$

$$k_y = k'_y \cos \theta + h (k'_x \sin \phi + k'_y k'_z \cos \phi) \quad (9)$$

$$k_z = k'_z \cos \theta - h (1 - (k'_z)^2) \cos \phi \quad (10)$$

where  $h = \sin \theta / \sqrt{1 - (k'_z)^2}$ .

Repeating iteratively this process, the complete trajectory of a photon travelling through the atmosphere can be reconstructed without using any extra restrictive approximation.

Figure 3 shows a trajectory of an arbitrary test solar photon since it enters at the top of the atmosphere (TOA) until it escapes again to the outer space. At each point  $P_i$ , the photon is scattered from the incident direction  $(\theta_{i-1}, \phi_{i-1})$  to the new direction  $(\theta_i, \phi_i)$ .  $(\vartheta_i, \varphi_i)$  are the scattering angles with respect to the incident angles. Figure 3 also shows the intersection points  $D$  used for photon counting at the reference level  $z_j$ .

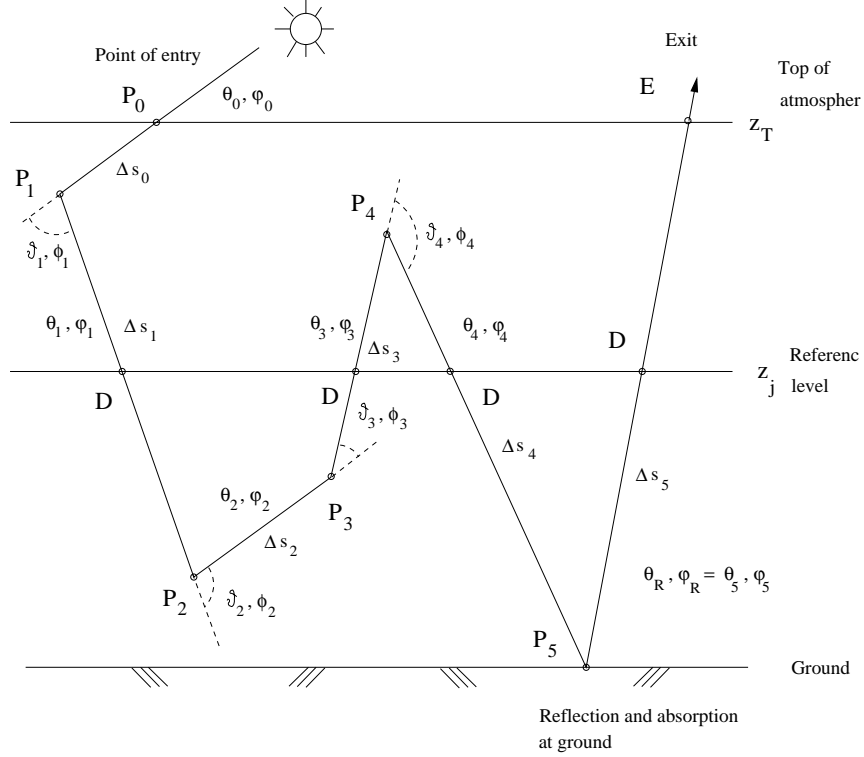


**Figure 3:** Trajectory of an arbitrary test photon

## 2.2 Treatment of Absorption and Selection of Scattering Type

Given an extinction event, the probability of a photon being absorbed is  $(1 - \omega_0)$ , where  $\omega_0$  is the single scattering albedo. The algorithm of the model could be designed in such a way that it follows the trajectory of the photon until it is absorbed or leaves the atmosphere (at the top or the the ground), and repeats the process for a huge number of photons. However, it is more efficient if one assigns a weight to a model photon (which represents a packet of photons), considers that only scattering takes place in the atmosphere and reduces the weight a quantity  $(1 - \omega_0)$  at each scattering event—in case that the photon reaches the Earth's surface,  $\omega_0$  has to be replaced by the ground albedo  $A_s$ . In this way, the effect of gaseous and particulate absorption can be determined after the photon trajectories in a purely scattering atmosphere have been computed, if the information about absorbed energy as a function of location have been conveniently stored.

Photons can interact in different ways with the atmosphere. Now, we wish to decide what kind of interaction takes place at each extinction point. Let the total extinction coefficient be the sum of all absorption and scattering coefficients,

$$\beta_{e,tot}(z) = \beta_{a,gas}(z) + \beta_{s,ray}(z) + \beta_{s,cld}(z) + \beta_{a,cld}(z) + \beta_{a,aer}(z) + \beta_{a,aer}(z)$$

where the subscripts 'e', 's' and 'a' make reference to extinction, scattering and absorption; and 'gas', 'ray', 'cld' and 'aer' to gas, Rayleigh, cloud and aerosol, respectively. In order to select which kind of interaction occurs, we use a new random number  $R[0, 1)$ . If

$$0 \leq R[0, 1) \leq \frac{\beta_{s,ray}(z)}{\beta_{e,tot}(z)} \quad (11)$$

then Rayleigh scattering is assumed to happen. If

$$\frac{\beta_{s,ray}(z)}{\beta_{e,tot}(z)} \leq R[0,1] \leq \frac{\beta_{s,ray}(z) + \beta_{s,cld}(z)}{\beta_{e,tot}(z)} \quad (12)$$

is the case, cloud droplet scattering will take place. In case that

$$\frac{\beta_{s,ray}(z) + \beta_{s,cld}(z)}{\beta_{e,tot}(z)} \leq R[0,1] \leq \frac{\beta_{s,ray}(z) + \beta_{s,cld}(z) + \beta_{s,aer}(z)}{\beta_{e,tot}(z)} \quad (13)$$

the photon will be scattered by aerosol particles. It can also happen that

$$\frac{\beta_{s,ray}(z) + \beta_{s,cld}(z) + \beta_{s,aer}(z)}{\beta_{e,tot}(z)} \leq R[0,1] \leq 1 \quad (14)$$

and in this case either gas, droplet or aerosol absorption is assumed to occur and the test photon will continue to the next extinction event without any change in flight direction.

### 2.3 Computation of the Flux Densities and Radiation Fields

The upward and downward flux densities,  $F^\uparrow(\theta_0; x, y, z)$  and  $F^\downarrow(\theta_0; x, y, z)$ , are easily computed by summing the photons up, or as in our case, by summing the weight of the model photon each time it crosses a horizontal test surface. If photon's direction is within the lower  $2\pi$  hemisphere its contribution is added to the downward flux density  $F^\downarrow$ , if it is within the upper  $2\pi$  hemisphere, it contributes to the upward flux density  $F^\uparrow$ .

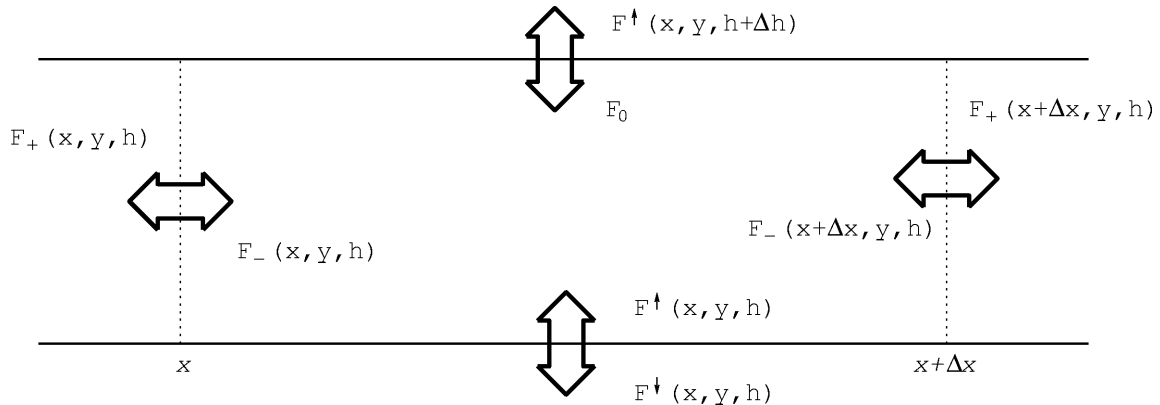


**Figure 4:** Radiative transfer in an atmospheric cell.

Transmission  $T$  and reflection  $R$  functions can be calculated straightforwardly as they are the normalized  $F^\uparrow$  and  $F^\downarrow$  flux densities to the incoming energy. Let us consider the energy balance in an atmospheric cell (see figure 4) (see also *Titov* [1998]). According to the law of energy conservation, the incoming energy must equal the outgoing plus the absorbed energy within the cell,

$$F_0 + F^\uparrow(x, y, h) = F^\uparrow(x, y, h + \Delta h) + F^\downarrow(x, y, h) + A'(x, y, h) + H'(x, y, h) \quad (15)$$

where  $F_0$  is the solar flux density,  $F^\uparrow$  and  $F^\downarrow$  are the upwelling and downwelling flux densities, respectively;  $H'$  is the horizontal flux density and  $A'$  is the absorbed power in the

cell. If we now refer all the quantities in Eq. (15) to the incoming power  $F_0 + F^\uparrow(x, y, h)$ , we can write the law of energy conservation in the form,

$$R(x, y) + T(x, y) + A(x, y) + H(x, y) = 1 \quad (16)$$

where  $R$  is the albedo,  $T$  is the transmittance,  $A$  is the absorptance and  $H$  the normalized net horizontal flux.

### 3 The Leipzig Monte Carlo Model (LMCM)

The LMCM takes into account the following wavelength dependent radiative processes in the solar spectral region: Rayleigh scattering by air molecules, scattering and absorption by both, aerosol particles and droplets, and absorption by several atmospheric gases ( $O_3$ ,  $O_2$ ,  $H_2O$ ,  $NO_2$ , etc). The gas absorption coefficients are pre-calculated with a Fortran code for arbitrary standard atmospheric profiles (tropical, polar, subpolar, etc.) of temperature, pressure and species mixing ratio, using the absorption cross section values of the different species published in the high-resolution transmission molecular absorption data base HITRAN (*Rothman et al.* [1998]) and other data references. In order to deal with the complicated line absorption spectrum of water vapor, we pre-compute the absorption coefficient for a certain wavelength interval by means of a line-by-line transmission code. We generate  $k$ -distribution fits as a function of temperature, air pressure and molecule concentration of water vapor. The result of these fits is stored and can be re-used for generating absorption coefficients as a function of the water vapor amount  $u$ .

In addition to the absorbing gases, the LMCM can deal with cloud and aerosol fields provided by cloud generators (Large Eddy Generators, fractal generators) or from measurement campaigns (Baltex Bridge Campaigns *BBC* and *BBC2*).

The treatment of the scattering cross section is of special interest in the radiative transfer modelling. If the medium under consideration is smoothly variable, and we attempt to obtain directionally averaged radiative quantities only, the Henyey-Greenstein phase function is a good approximation to the Mie-scattering phase function:

$$p_{HG}(\cos \Theta) = \frac{1 - g^2}{(1 + g^2 - 2g \cos \Theta)^{3/2}}, \quad (17)$$

where  $\Theta$  is the scattering angle, and  $g$  is the asymmetry parameter (*Thomas and Stamnes* [1999]). However, for a more accurate treatment of Mie scattering, a tabulated phase function is required. The LMCM can select between the two cases depending on the needs.

The LMCM can be run in three different modes:

- The independent pixel approximation (IPA) mode, which considers 3D variability of the optical property fields but does not allow the radiative horizontal transport between the individual columns,
- the two-dimensional mode (2D), which accounts for the variability in only one horizontal direction but allowing for horizontal transport,
- and the three-dimensional mode (3D), which considers the most general case: 3D variability with radiative transfer in all directions.



According to the difficulty of the problem and the inhomogeneity of the cloud fields under study, the different running modes will be selected in order to optimize the achieved accuracy with respect to the running time.

At the moment, the LMCM yields horizontal and vertical flux densities, and actinic fluxes at arbitrary surfaces as well as power absorption in arbitrary cells. Transmittance, reflectance, absorptance and heating rates are also directly derived.

## 4 Radiative Transfer Simulations

In this chapter, the results of several simulations with the LMCM are presented. In order to validate our model, two cloud fields of the I3RC project have been used as inputs. The model results are compared with those ones obtained with other internationally accepted models. We can see in the following sections that the agreement of the radiative fields calculated by LMCM with the other models is very good, confirming its reliability for RT computations.

### 4.1 Intercomparison of 3D Radiation Codes (I3RC)

This project was conceived with the goal of comparing a wide variety of three-dimensional radiative transfer methods applied to Earth's atmosphere, with a few selected cloud fields as input, and a few selected radiative quantities as output. I3RC is proceeding in three phases. During Phase I, now complete, several baseline radiative computations for 3D radiative transfer through Earth atmospheric clouds were defined, based upon three cloud fields: a 1D academic 'step' cloud field, a 2D field derived from the ARM cloud radar, and a 3D field derived from radiances measured by the Landsat 5 Thematic Mapper instrument.

We have fully performed the simulations suggested in phase I of I3RC and some selected results for the last two cases will be presented next.

#### 4.1.1 ARM Radar Reconstructed Cloud

The 2D cloud field for this experiment is based on extinction retrievals from the MMCR (Millimeter Cloud Radar) and the MWR (microwave radiometer) at the ARM CART site in Lamont, Oklahoma on February 8, 1998.

The field consists of 640 columns along the x-direction, which were set to have a 50 m horizontal width (for the 10 sec. measurements this corresponds to the observed wind speed of  $\sim 5$  m/s), and each column is resolved into 54 vertical layers which are 45 meters thick (z-direction). The optical depth field is illustrated in figure 5, where one can see that it extends vertically from circa 0.6 km to 2.43 km above the Earth's surface.

In order to be sure that all the models calculate the same quantities, with the same conditions, the same assumptions are taken in every computation. For the RT calculations presented here, the following assumptions were made:

- 1) cloud infinite along the y-direction,
- 2) no atmospheric effects
- 2) periodic boundary conditions (cloud field is repeated an infinite number of times along the x direction),

- 3) black surface, *i.e.* surface albedo ( $A_s$ ) of 0,
- 4) Henyey-Greenstein phase function (PF) with  $g=0.85$ ,
- 5) single scattering albedo ( $\omega_0$ ) of 0.99, and
- 6) solar zenith angle ( $\theta_0$ ) of  $60^\circ$ .

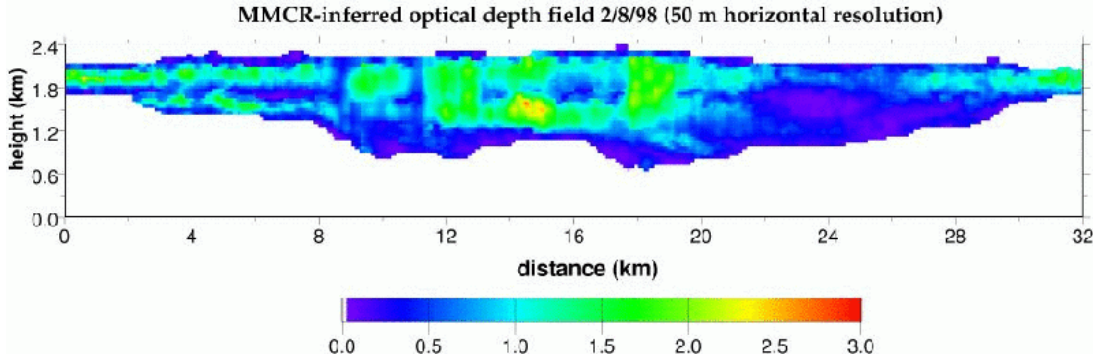


**Figure 5:** ARM radar reconstructed cloud. Case 2 of phase I of the I3RC project.

Several institutions took part in I3RC project with different methods, but we will only show the results of three of them together with our own ones. The I3RC's participants selected are: The National Center for Atmospheric Research (*NCAR*), University of Colorado (SHDOM) (*Evans [1998]*) and the Institute for Marine Research at the University of Kiel (UNIK). The abbreviations are the same as in the I3RC web page. NCAR and UNIK (*Scheier [2001]*) participate with MC codes, whereas the University of Colorado does with a RTE-integration method, the so called Spherical Harmonic Discrete Ordinate Method.

Figure 6 illustrates xy-plots showing the value of the radiative quantity (reflectance, transmittance, absorptance and horizontal flux density) vs. location (for a 3.2 km segment), using the assumptions previously mentioned. For all computations, albedo and transmittance are registered at cloud boundaries. For this case, cloud top is defined as the topmost level for which a cloud cell with non-zero extinction is encountered (2.43 km), and cloud base is defined as the last level where a cloudy cell is encountered (0.63km). One can see that the agreement of LMCM with the other codes is fully acceptable for all radiative quantities.

In figure 7, the domain-averaged values of the radiation fields are compared. One can see that all radiative codes are in very good agreement (better than 0.1 %).

#### 4.1.2 3D Marine Boundary Layer Cloud

For the next computations we have chosen the case 3 of the Phase I of the I3RC project. This 2D cloud field stems from an Independent Approximation retrieval on a 128x128 segment of a Landsat-4 scene. For the retrievals, the ocean surface albedo was set 0.043. Liquid water phase was assumed throughout, and a lognormal drop size distribution with effective radius of  $10 \mu m$  and effective variance of 0.15 was used to construct the look-up tables. Any other atmospheric effect was neglected in the retrievals.

The optical depth field consists of 128 vertically homogeneous pixels along the x- and y-directions, with a horizontal width of 30 m in both directions (see figure 8). In order

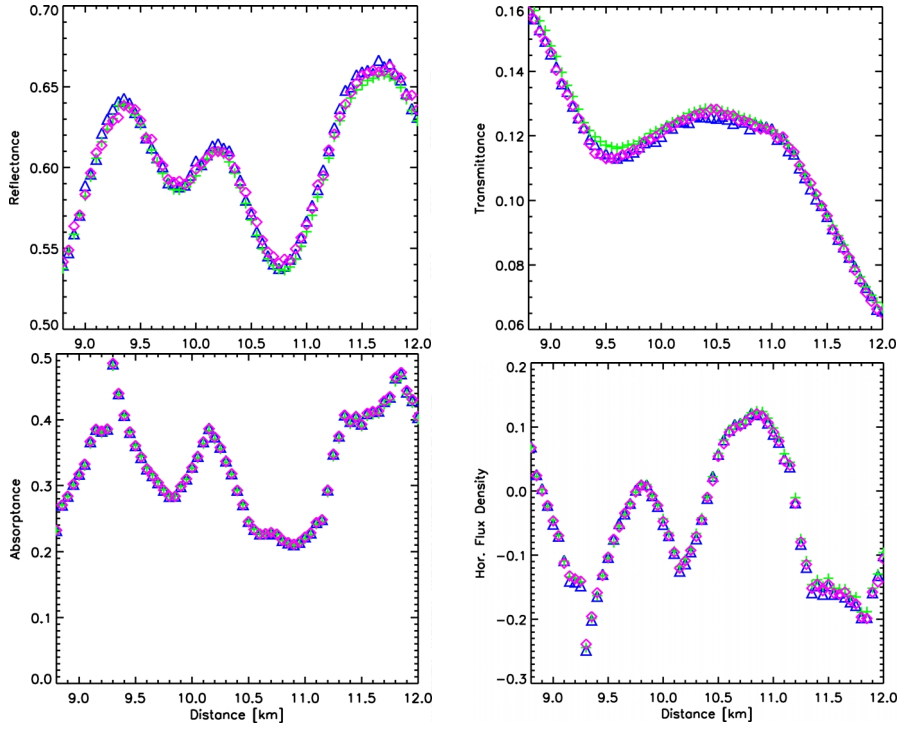


**Figure 6:** Illustration of several radiative quantities —albedo (upper left), transmittance (upper right), absorptance (lower left) and net horizontal flux density (lower right)— calculated with different models: +: NCAR,  $\Delta$ : SHDOM,  $\diamond$ : LMCM, for the cloud field of the case 2, phase I of I3RC project. Solar zenith angle was set to  $60^\circ$  and single scattering albedo to 0.99.

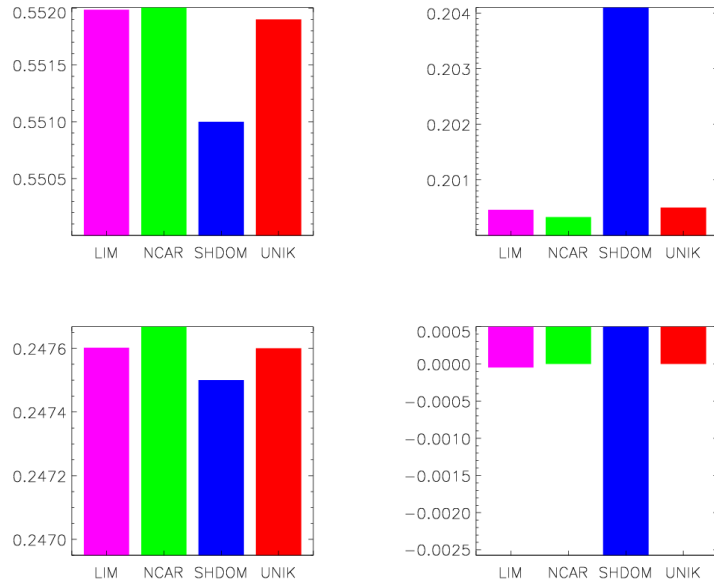


**Figure 7:** Box plots showing means of the various radiative quantities —albedo (upper left), transmittance (upper right), absorptance (lower left) and net horizontal flux density (lower right)— for the same cloud field and conditions as in figure 6. LMCM results are denoted with LIM (Leipzig Institute of Meteorology).

to build up a 3D spacial cloud field, a flat cloud bottom at 0.2 km was considered and cloud top heights were determined from the geometrical thickness field. The mean cloud optical depth (cloudy part) is 11.4 and the standard deviation is 10.6; the cloud fraction is 0.884.

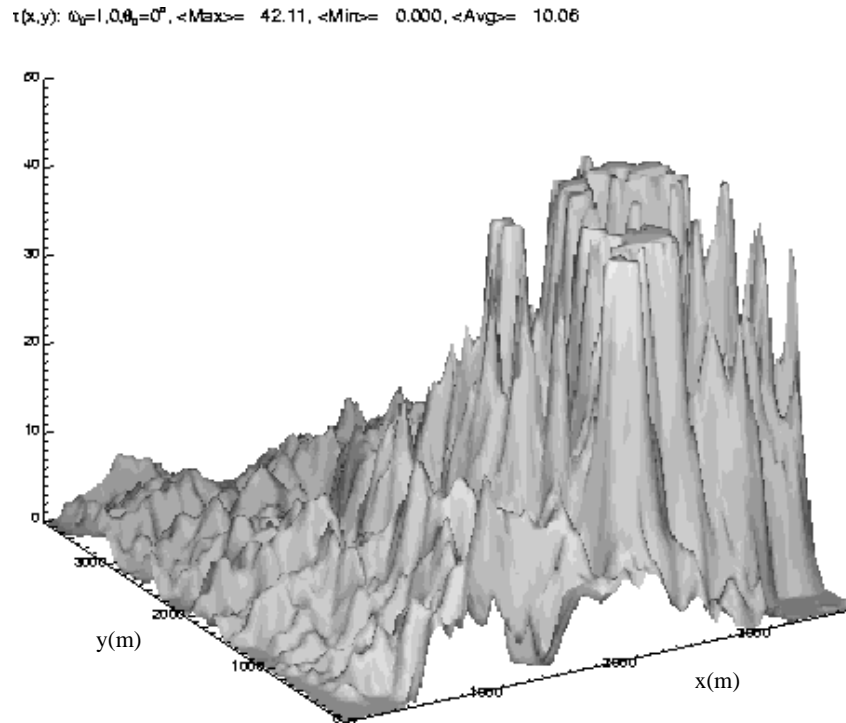


**Figure 8:** Illustration of the optical depth field of the 3D marine boundary layer cloud used in case 3 of phase I of I3RC project.

As in this experiment the extinction field is three-dimensional, it is necessary to compare the two-dimensional radiative quantities in separate graphs. Only the comparison of LMCM results with those of our 4DCLOUDS-project partner UNIK are shown (see figure 9). Although the extinction field is highly variable and the solar illumination is not perpendicular, the figures provided by both methods seem to be twins. The mean, maximal and minimal values agree better than 0.1 %, which is clearly better than the required accuracy in the I3RC project.

## 5 Conclusions and outlook

In this paper, it has been briefly described the MC method as an efficient tool to deal with the radiative transfer in the atmosphere. A new code, the LMCM, based on this approach has been presented and it fully succeeded in the results' comparison with results from other accepted codes. Having the proof of the validity of LMCM, this model will be employed together with the models GRIMALDI (UNIK) and SHDOM for future radiative research scheduled in context of the 4DCLOUDS project.

Currently, radiative calculations with a radar/microwave composite cloud measured in the BBC experiment are being carried out. Sensitivity studies with ideal clouds have been done to select flight paths for the aircraft radiation and microphysics measurements in the next campaign (BBC2) to be performed by the Institute for Tropospheric Research (IfT, Leipzig).

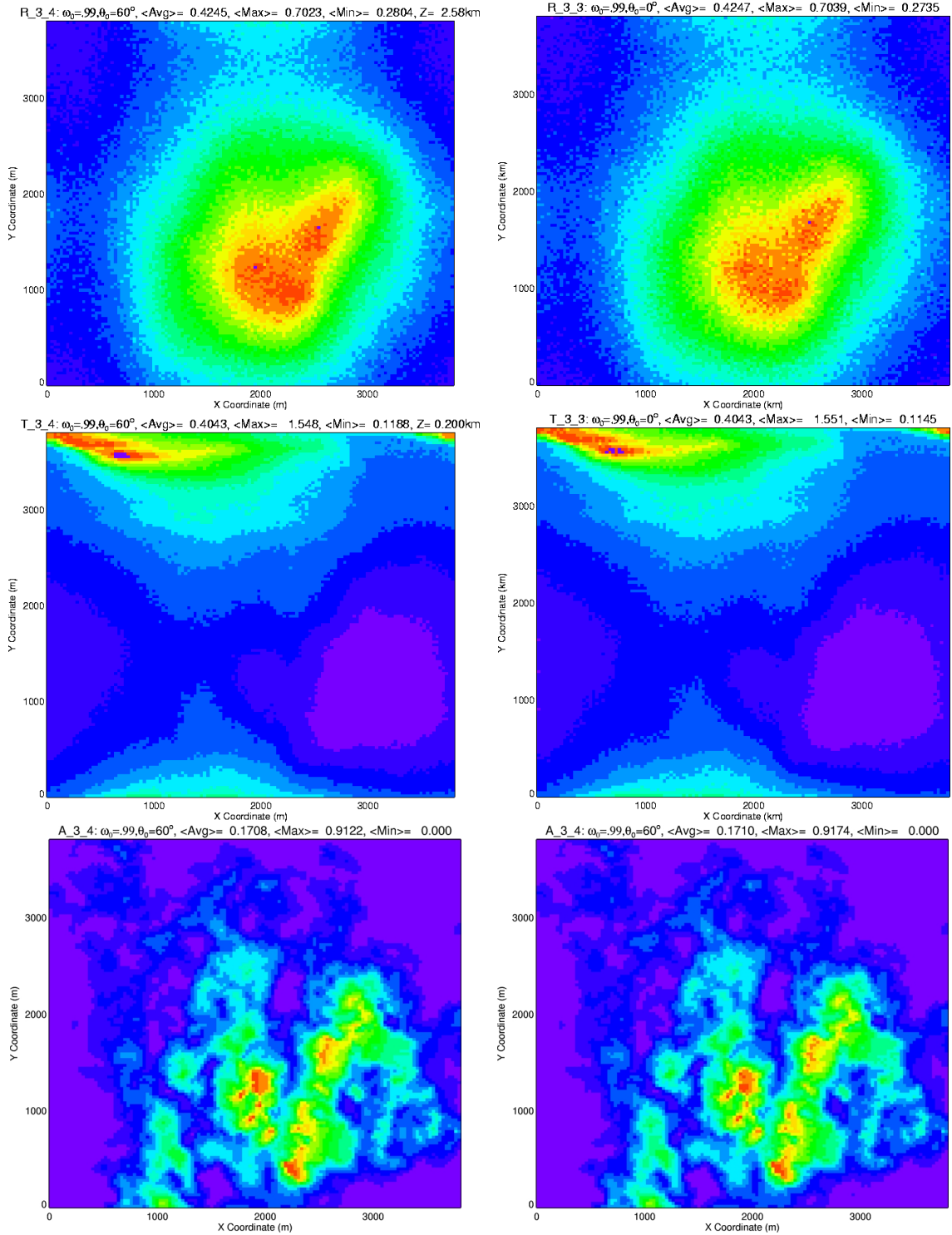


**Figure 9:** Illustration of several radiative quantities —albedo (upper), transmittance (middle), absorptance (lower)— computed by LCMC (left) and UNIK (right), for the cloud field of the case 3, phase I of I3RC project. Solar zenith angle was set to  $60^\circ$  and single scattering albedo to 0.99.

In the near future, radiative transfer simulation using cloud fields from in situ aircraft microphysics measurement as input, will be compared with the yields of the aircraft radiometers.

## Acknowledgments

This research project is funded by the Bundesministerium für Bildung und Forschung (BMBF) within the research programme AFO2000.

## References

4DCLOUDS project, general description:

<http://www.meteo.uni-bonn.de/projekte/4d-clouds/description/4d-clouds/>

BBC, Baltex Bridge Campaign:

<http://www.meteo.uni-bonn.de/projekte/4d-clouds/bbc/>

BBC2, Baltex Bridge Campaign 2:

<http://www.meteo.uni-bonn.de/projekte/4d-clouds/bbc2/>

Cess, R. D., E. D. Dutton, J. J. DeLuisi and F. Jiang, 1996: Absorption of solar absorption by clouds: Interpretation of satellite, surface, and aircraft measurements, *J. Geophys. Res.*, **101**, 23,299-23,309.

Evans K. F., 1998: The Spherical Harmonics Discrete Ordinate Method for Three-Dimensional Atmospheric Radiative Transfer. *J. Atmos. Sci.*, **55**, 429-445.

I3RC, The Intercomparison of Three-Dimensional Radiative Codes project: <http://climate.gsfc.nasa.gov/I3RC/>

Marchuk G. I., G. A. Mikhailov, M. A. Nazarialiev, R. A. Darbinjan, B. A. Kargin and B. S. Elepov, 1980: The Monte Carlo Methods in Atmospheric Optics. Springer-Verlag Berlin Heidelberg New York.

NCAR, National Center for atmospheric Research:

<http://www.ncar.ucar.edu/ncar/>

Rothman, L. S., et al., 1998: The HITRAN molecular spectroscopic database and HAWKS (HITRAN atmospheric workstations): 1996 edition, *J. Quant. Spectrosc. Radiat. Transfer*, **60**, 665-710.

Scheirer, R., 2001: Solarer Strahlungstransport in der inhomogenen Atmosphäre. Berichte aus dem Institut für Meereskunde, Christian-Albrechts-Universität Kiel, 123 p.

<http://www.ifm.uni-kiel.de/fb/fb1/me/research/Projekte/RemSens/SourceCodes/codes.html>

Titov G. A., 1998: Radiative Transport and Absorption in Stratocumulus Clouds. *J. Atmos. Sci.*, **55**, 2549-2560.

Thomas G. E. and K. Stamnes, 1999: Radiative Transfer in the Atmosphere and Ocean. Cambridge University Press.

Trautmann T., I. Podgorny, J. Landgraf and P.J. Crutzen, 1999: Actinic fluxes and dissociation coefficients in cloud fields embedded in realistic atmospheres. *J. Geophys. Res.*, **104**, 30,173-30,192.

Valero F. P. J., R. D. Cess, M. Zhang, S. K. Pope, A. Bucholtz, B. Bush and J. Vitko Jr., 1997: Absorption of solar radiation by cloudy atmosphere: Interpretation of collocated aircraft measurements. *J. Geophys. Res.*, **102**, 29,917-29,927